Analysis of the Reverse Flow Chromatographic Reactor

Hugo S. Caram and Guillermo A. Viecco
Dept. of Chemical Engineering, Lehigh University, Bethlehem, PA 18015

DOI 10.1002/aic.10194
Published online in Wiley InterScience (www.interscience.wiley.com).

A reverse flow chromatographic reactor with side feed (RFCR) can be used to improve the conversion and selectivity for irreversible and reversible reaction systems beyond the values obtained from conventional steady-state reactors in the case where the reactants are more strongly adsorbed than the products. It is also simpler than conventional chromatographic, moving, and simulated moving beds and other systems that combine reaction and adsorption separation. The results of the study show the robustness and stability of the system, as well as its capacity to significantly improve conversion and selectivity for several reaction systems, including consecutive reactions. Simulation results of this mathematical model for the hydrogenation of 1,3,5-trymethylbenzene (MES) compare well with previous studies, using countercurrent moving-bed reactors and simulated countercurrent bed reactors. © 2004 American Institute of Chemical Engineers *AIChE J,* 50: 2266–2275, 2004

Introduction

In most chemical processes, the chemical reaction itself is only one of several processes taking place. There are often internal and external separation and heat exchange processes, which are of critical importance for the reaction performance and in the subsequent processing steps. In view of this complex picture, reaction engineering has shifted from conventional - batch, perfectly mixed stirred tank, and plug flow - reactors operating under steady state to multifunctional and/or transient reactors. These new type of reactors take advantage of the coupling of several operations into a single equipment, and the transient behavior of them, to improve in characteristics, such as yield, productivity, flexibility, safety, and investment and operation costs.

Among these multifunctional reactors, the chromatographic reactor (see Figure 1), which couples chemical reaction and adsorptive separation, has received a great deal of attention since 1960. The importance of the chromatographic reactor is due to its very simple and attractive principle: the continuous separation of products can drive a reversible reaction to near completion since it suppresses the rate of the reverse reaction and, at the same time, high purity products are obtained. Initially, chromatographic reactors were operated by injecting single pulses of reactant into the column, leading into batch operation with high product purity and conversion, but with low productivity. Therefore, the first application of the pulse chromatographic reactor was as a tool for obtaining kinetic data and determining reaction mechanisms for heterogeneous catalytic reactions. Coca and Langer (1983) reviewed the mathematical models used to obtain kinetic data, and presented some of the reactions that have been studied.

In order for the chromatographic reactor to have industrial applications, continuous operation had to be achieved. Several different schemes have been developed over the years: periodic pulsing, rotating, countercurrent, simulated countercurrent, and reverse flow. The first approach to obtain continuous operation was developed by Matsen et al. (1965). In this article, periodic pulsing of the reactant was used (instead of a single pulse) to carry out the catalytic dehydrogenation of cyclohexane. Later, Gore (1967) studied the effect of the pulse shape and the frequency of the pulsing in the operation of the chromatographic reactor. Schweich and Villermaux (1978) assumed

Correspondence concerning this article should be addressed to H. S. Caram at hsc0@lehigh.edu.

local chemical equilibrium and used the plate theory to describe the chromatographic reactor with pulse feed, and in 1982 compared their mathematical model with experimental data. Mile (1982) studying the dehydrogenation of cyclohexane under periodic pulsing, found that high carrier flow rates give good separation but poor conversions, while for low carrier flow rates the separation is poor and only the equilibrium yield can be attained. Between these two extremes, there is an optimal residence time, long enough for the system, not to be limited kinetically, but with flow high enough to assure separation of the products. This conclusion is of critical importance for the reverse flow chromatographic reactor, as it will be discussed later.

An alternative to the periodic pulsing of reactant was developed by Cho et al. (1980), who successfully carried out the acid catalyzed hydrolysis of methyl formate in a continuous flow annular reactor, with rotating feed and collecting points. Matsen (1968) introduced the countercurrent moving-bed chromatographic reactor (CMCR) (see Figure 2), a chromatographic system where the fluid and the solid phases flow countercurrent to each other past a fixed feed point, obtaining continuous feed of the reactant and separation of the products. The majority of the early research on the CMCR was concerned with the development of mathematical models. Takeuchi and Uragachi (1976, 1977a) studied the effect of feeding the reactant at different points of the bed, as well as the effect of the CMCR on the selectivity for consecutive reactions. Among the few experimental studies that were carried out in the CMCR was the irreversible catalytic oxidation of CO over Al_2O_3 by Takeuchi and Uragachi (1977b), and the reversible catalytic hydrogenation of 1,3,5 trimethylbenze by Petroulas et al. (1985).

The operation of the CMCR presents problems, such as channeling, abrasion, attrition, and fines removal. These

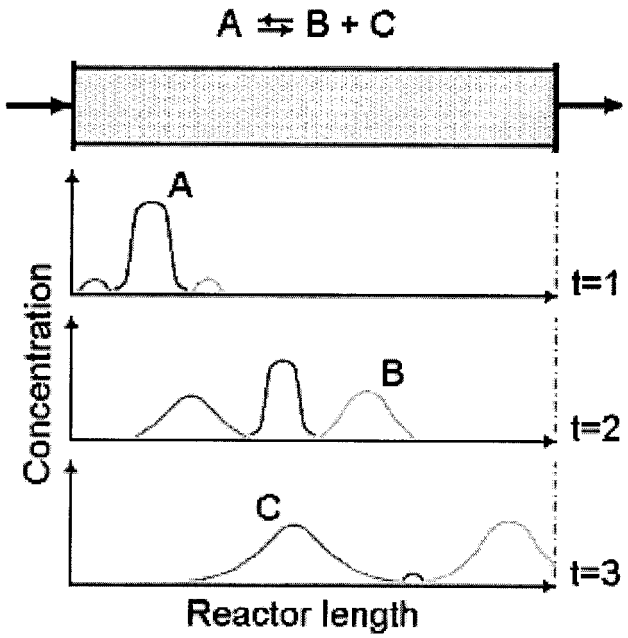

Figure 1. Concentration profiles in a chromatographic reactor where a single pulse of reactant A is fed.

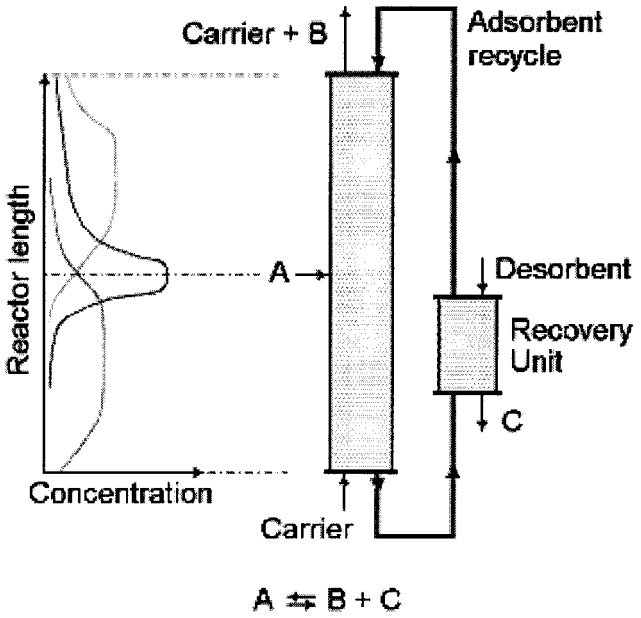

Figure 2. CMCR and expected concentration profiles for a reversible reaction.

C is strongly adsorbed, while B is weakly adsorbed.

problems can be avoided by moving the feed and removal points to simulate countercurrent movement of the fluid and solid phases. This lead to the development of the simulated countercurrent moving-bed chromatographic reactor (SCMCR) (see Figure 3). The simplest configuration of the SMCR is the single column SCMCR, where the reactant feed point is moved along a fixed bed in the same direction as the fluid flow but at a lower speed. If the feed point were to move continuously along the bed, this would exactly simulate the CMCR. Because of the discrete feed and exit pints used in practice, the product profile for the SCMCR will be approximately a step function. If the single column SCMCR is divided at the feed point into several smaller columns with inlet and outlet ports between columns, one arrives to the multicolumn SCMCR. The multicolumn SCMCR was found out to be a more convenient way to carrying out laboratory investigations. The multicolumn SCMCR has received a great deal of attention since its introduction, and has been applied to the oxidative coupling of methane (Kruglov et al., 1996), to esterifications (Mazzotti et al., 1996; Kawase et al., 1996; Kawase et al., 1999;), to the synthesis of bioproducts (Barker et al., 1992; Azevedo and Rodrigues, 2001; Kawase et al., 2001), among other applications.

The reverse flow chromatographic reactor (RFCR) is a packed bed that can be packed with adsorbent, or with and admixture of adsorbent and catalyst, where at least one of the reactants is fed at the middle of the reactor, and where the flow direction of the carrier is periodically switched according to Figure 4. If the adsorbent has a high adsorption capacity toward the reactant, and low toward the products, the periodic switching of the carrier traps the strongly adsorbed reactant inside the reactor. The value of the RFCR can be illustrated for the reversible first-order reaction $A \rightleftarrows B$. If the adsorbent has a

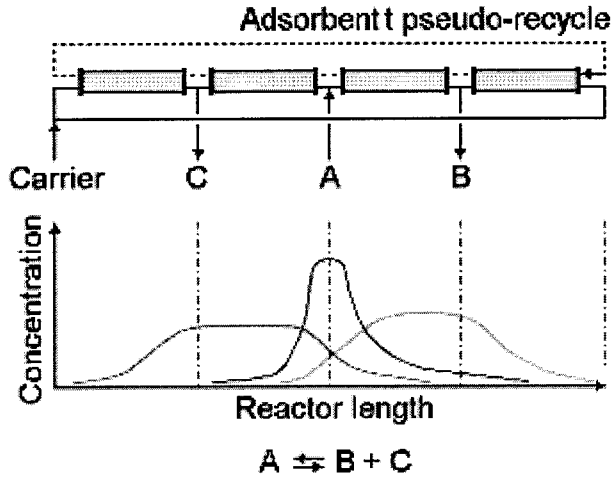

Figure 3. Multicolumn SCMCR and expected concentration profiles for a reversible reaction.

C is strongly adsorbed, while B is weakly adsorbed.

lower adsorption capacity toward the product than the reactant, then the residence time of the product will be reduced, and the reverse reaction is inhibited by fast removal of the reaction products, allowing higher overall conversions than the equilibrium value.

The use of reverse flow of the carrier fluid in chromatographic reactors has only received attention by a group of investigators in Europe. Agar and Ruppel (1988) and Falle et al. (1995) used the adsorption capacity of the chromatographic stationary phase and the wrong way phenomena (Matros, 1989) to propose a reactor with side feed and periodic flow reversal to carry out the selective catalytic reduction of NO_x with high NO_x conversion, and no escape of ammonia from the reactor. Their model only considered the adsorption of ammonia to the catalyst, and special attention was given to the shape and velocity of the ammonia wave.

In the current study, the RFCR has been further studied and several advantages over conventional steady-state and chromatographic reactors have been found. Thanks to the high concentration of reactant within the reactor, which can exceed the feed concentration, faster reaction rates are obtained, and as a result, shorter reactors are required compared to CMCR and SCMCR. Although conversion and selectivity are improved over conventional steady-state reactors, and conversion is similar to that of CMCR, purity of the products is reduced. However, partial separation of

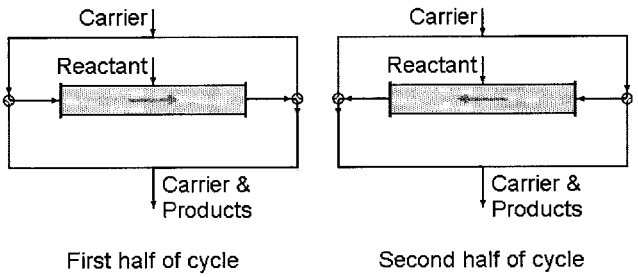

Figure 4. Representation of a RFCR.

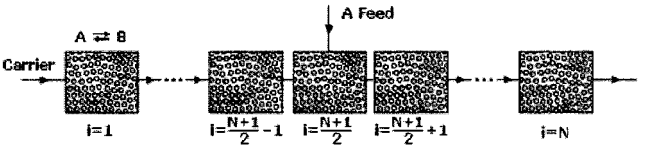

Figure 5. The RFCR represented as a series of CSTRs.

products in reversible reactions with more than one product can be obtained by splitting the exit stream into different vessels at different times. Also, for consecutive reactions, selectivity and yield are improved when the main product has a lower adsorption capacity than the reactant.

Mathematical Model

A preliminary evaluation of the performance of the reactor can be obtained modeling the RFCR as a chain of N (odd) continuous stirred-tank reactors (CSTR). The tank in series model has been used to represent two effects, the axial mixing and the interfacial mass-transfer resistance between the solid and fluid phase. No effort is made in this article to relate the number of stages to a physical parameter, and the number of stages is left as an adjustable parameter. The model assumes that the reactor is isothermal, with negligible pressure drop, and the reactant is fed at the $^{(N+1)}/_{2}$ CSTR. The complete cycle is split into a forward cycle, where carrier fluid enters at the 1st CSTR and leaves at the Nth CSTR, and a reverse cycle. For a first-order irreversible reaction $A \xrightarrow{k_f} B$, the material balance at the ith CSTR in the forward cycle for component A is

$$\varepsilon V_i \frac{dC_i}{dt} + (1-\varepsilon)V_i \frac{dC_{i,s}}{dt} = q(C_{i-1} - C_i) - V_i k_f C_i \quad (1)$$

If local adsorption equilibrium between the two phases exist at each CSTR, and if the adsorption equilibrium can be described by linear adsorption isotherm, $C_{i,s} = K_A C_i$, then the concentration in the stationary phase can be eliminated from Eq. 1, yielding

$$(\varepsilon + (1-\varepsilon)K_A)V_i \frac{dC_i}{dt} = q(C_{i-1} - C_i) - V_i k_f C_i \quad (2)$$

Defining

$$K'_A = \varepsilon + (1-\varepsilon)K_A \quad (3)$$

Eq. 2 can be written in dimensionless variables as

$$\frac{dC_i}{d\tau_i} = C_{i-1} - C_i - Da_i C_i \quad (4)$$

where

$$\tau_i = \frac{tq}{K'_A V_i} \quad (5a)$$

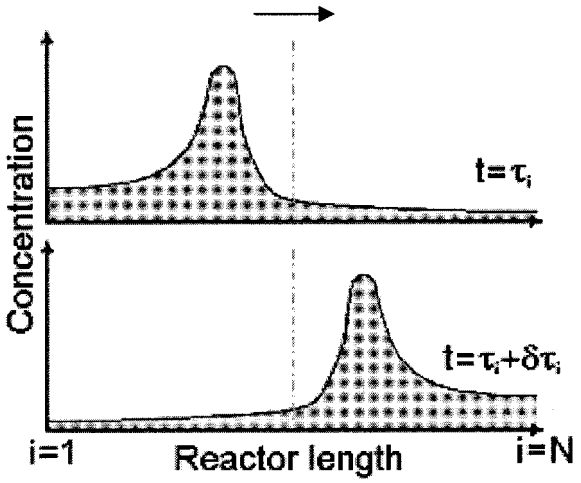

Figure 6. Concentration profile as a function of the reactor number at the start ($\tau_i = 0$) and at the end of half a cycle ($\tau_i = \delta\tau_i$).

The arrow shows the flow direction.

$$Da_i = \frac{V_i k_f}{q} \tag{5b}$$

For N CSTRs with the same volume, the resulting system of ODEs for the concentration vector $\mathbf{C}=[C_1,C_2,\ldots,C_N]^T$ can be written in matrix form as

$$\frac{d\mathbf{C}}{d\tau_i} = \mathbf{AC} + \mathbf{F} \tag{6}$$

where the coefficient matrix **A,** and the feed vector **F** are

$$\mathbf{A} = \begin{bmatrix} -(1+Da_i) & & & 0 \\ 1 & -(1+Da_i) & & \\ & \ddots & \ddots & \\ 0 & & 1 & -(1+Da_i) \end{bmatrix} \tag{7a}$$

$$\mathbf{F} = \begin{bmatrix} 0 \\ \vdots \\ 0 \\ C_{A,F} \\ 0 \\ \vdots \\ 0 \end{bmatrix} \leftarrow \frac{N+1}{2} \tag{7b}$$

For initial conditions given by $\mathbf{C}_0$, the solution to this problem is widely known

$$\mathbf{C}(\tau_i) = e^{\mathbf{A}\tau_i}\mathbf{C}_0 + \mathbf{A}^{-1}[e^{\mathbf{A}\tau_i} - \mathbf{I}]\mathbf{F} \tag{8}$$

At the cyclic steady state, the concentration at the beginning of the cycle is the mirror image of the concentration at the end of half the cycle (Figure 6). Therefore

$$\mathbf{C}_0(\tau_i) = \mathbf{M}\mathbf{C}_0(\tau_i + \delta\tau_i) \tag{9}$$

where $\delta\tau_i$ is the dimensionless half cycle time, and **M** is the mirror matrix given by

$$\mathbf{M} = \begin{bmatrix} 0 & & 1 \\ & \iddots & \\ 1 & & 0 \end{bmatrix} \tag{10}$$

Substituting Eq. 9 into 8, and rearranging the initial concentration at the cyclic steady state, is then given by

$$\mathbf{C}_0 = [\mathbf{M} - e^{\mathbf{A}\delta\tau_i}]^{-1}\mathbf{A}^{-1}[e^{\mathbf{A}\delta\tau_i} - \mathbf{I}]\mathbf{F} \tag{11}$$

Finally, the average concentration of the reactor can be obtained by

$$\mathbf{C}_{average} = \frac{1}{\delta\tau_i}\int_0^{\delta\tau_i} \mathbf{C}(\tau_i)d\tau = \frac{\mathbf{A}^{-1}}{\delta\tau_i}[e^{\mathbf{A}\delta\tau_i} - \mathbf{I}]\mathbf{C}_0 + \frac{\mathbf{A}^{-2}}{\delta\tau_i}[e^{\mathbf{A}\delta\tau_i} - \mathbf{I}]\mathbf{F} - \mathbf{A}^{-1}\mathbf{F} \tag{12}$$

For consecutive reactions of the type, $A \xrightarrow{k_1} B \xrightarrow{k_f} C$, the material balance for component A and B in the forward cycle are

$$K'_A V_i \frac{dC_{A,i}}{dt} = q(C_{A,i-1} - C_{A,i}) - V_i k_1 C_{A,i} \tag{13a}$$

$$K'_B V_i \frac{dC_{B,i}}{dt} = q(C_{B,i-1} - C_{B,i}) + V_i k_1 C_{A,i} - V_i k_2 C_{B,i} \tag{13b}$$

In dimensionless variables, using the definitions of Eq 5a and 5b, the material balance is now

$$\frac{dC_{A,i}}{d\tau_i} = C_{A,i-1} - C_{A,i} - Da_i C_{A,i} \tag{14a}$$

$$\frac{dC_{B,i}}{d\tau_i} = \gamma C_{B,i-1} - \gamma C_{B,i} + \gamma Da_i C_{A,i} - \gamma\kappa Da_i C_{B,i} \tag{14b}$$

where

$$\gamma = \frac{K'_A}{K'_B} \tag{15a}$$

$$\kappa = \frac{k_2}{k_1} \tag{15b}$$

The **A** matrix for the ODE system is given by

$$\mathbf{A} = \begin{bmatrix} \begin{vmatrix} -(1+Da_i) & & 0 \\ 1 & \ddots & \\ 0 & 1 & -(1+Da_i) \end{vmatrix} & 0 \\ \begin{vmatrix} \gamma Da_i & & 0 \\ & \ddots & \\ 0 & & \gamma Da_i \end{vmatrix} & \begin{vmatrix} -\gamma(1+\kappa Da_i) & & 0 \\ \gamma & \ddots & \\ 0 & \gamma & -\gamma(1+\kappa Da_i) \end{vmatrix} \end{bmatrix} \tag{16}$$

and the mirror matrix, for a two-component system, is

$$\mathbf{M} = \begin{bmatrix} \begin{vmatrix} 0 & & 1 \\ & \iddots & \\ 1 & & 0 \end{vmatrix} & 0 \\ 0 & \begin{vmatrix} 0 & & 1 \\ & \iddots & \\ 1 & & 0 \end{vmatrix} \end{bmatrix} \tag{17}$$

For the reversible reaction the material balances for components A and B in the forward cycle are

$$K'_A V_i \frac{dC_{A,i}}{dt} = q(C_{A,i-1} - C_{A,i}) - V_i k_f \left(C_{A,i} - \frac{C_{B,i}}{K_{eq}} \right) \tag{18a}$$

$$K'_B V_i \frac{dC_{B,i}}{dt} = q(C_{B,i-1} - C_{B,i}) + V_i k_f \left(C_{A,i} - \frac{C_{B,i}}{K_{eq}} \right) \tag{18b}$$

In dimensionless variables Eq. 18, is

$$\frac{dC_{A,i}}{d\tau_i} = C_{A,i-1} - C_{A,i} - Da_i C_{A,i} + \frac{Da_i}{K_{eq}} C_{B,i} \tag{19a}$$

$$\frac{dC_{B,i}}{d\tau_i} = \gamma C_{B,i-1} - \gamma C_{B,i} + \gamma Da_i C_{A,i} - \gamma \frac{Da_i}{K_{eq}} C_{B,i} \tag{19b}$$

The dimensionless variables and parameters are given by Eqs. 5 and 15.a.

The **A** matrix is now

$$\mathbf{A} = \begin{bmatrix} \begin{vmatrix} -(1+Da_i) & & 0 \\ 1 & \ddots & \\ 0 & 1 & -(1+Da_i) \end{vmatrix} & \begin{vmatrix} Da_i/K_{eq} & & 0 \\ & \ddots & \\ 0 & & Da_i/K_{eq} \end{vmatrix} \\ \begin{vmatrix} \gamma Da_i & & 0 \\ & \ddots & \\ 0 & & \gamma Da_i \end{vmatrix} & \begin{vmatrix} -\gamma(1+Da_i/K_{eq}) & & 0 \\ \gamma & \ddots & \\ 0 & \gamma & -\gamma(1+Da_i/K_{eq}) \end{vmatrix} \end{bmatrix} \tag{20}$$

and the mirror matrix is given by Eq. 17.

In the development of the model, the dimensionless numbers were defined using the volume of a single CSTR. Since the total volume of the RFCR is the summation of the volume of all individual CSTRs, the dimensionless numbers can be redefined using now the total volume of the RFCR. This yields in

$$\tau = \frac{tq}{K'_A V} = \frac{tq}{K'_A N V_i} = \frac{\tau_i}{N} \tag{21a}$$

$$Da = \frac{Vk_f}{q} = \frac{NV_i k_f}{q} = NDa_i \tag{21b}$$

Although the model is derived for a homogeneous catalytic reaction, a heterogeneous catalytic reaction model can be easily constructed for a linear adsorption isotherm by considering the solid phase as an admixture of catalyst and adsorbent. The resulting model retains the linearity that allows for the analytical solution presented.

Results and Discussion

First-order irreversible reactions

For irreversible reactions, the conversion in a RFCR is a function of three dimensionless parameters: the "reactor size" *Da*; the switching time $\delta\tau^*$; and the number of equilibrium stages *N*; whereas for conventional reactors - batch, plug flow or a single CSTR - the conversion is only a function of the reactor size (*Da*). When irreversible reactions are carried out in a RFCR, the interaction between adsorption and periodic flow reversal of the carrier traps the reactant inside the reactor, increasing the residence time of the reactant without increasing the reactor size or decreasing the flow rate. This effect should increase the conversion for a first-order irreversible reaction in a RFCR compared with that of conventional reactors. In Figure

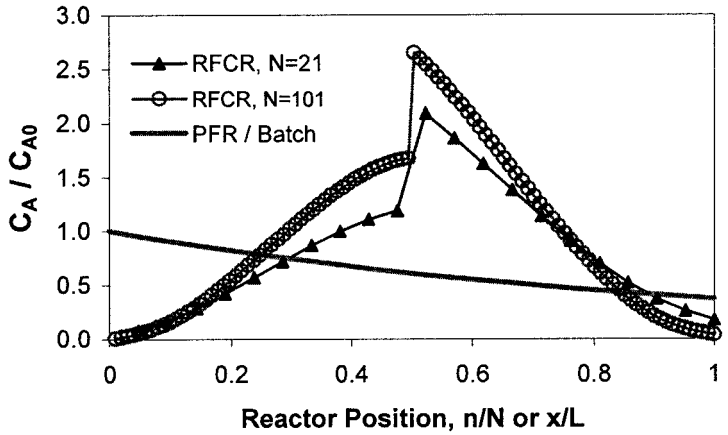

Figure 7. Average concentration profile for a PFR and for a RFCR for two different values of *N* during the forward cycle for the reaction A→B.

Da =1.0 for the PFR, and the RFCR and $\delta\tau^*$=0.4 for the RFCR.

7, the average concentration profile in a RFCR during the forward cycle is compared to the concentration of a plug-flow reactor (PFR) for the same reactor size (*Da*). In a PFR, the concentration continually decreases from the feed concentration to the exit concentration, whereas, for the RFCR, the concentration is lower at both ends of the reactor, but shows a spike around the feed CSTR, where it is higher than the feed concentration. Finally, the increase in the number of CSTRs (*N*), or equilibrium stages, increases both the concentration at the feed CSTR and the conversion.

Figure 8 shows the conversion as a function of the switching time for different reactor sizes. As the switching time decreases, the conversion increases until it reaches a plateau at very small switching times. At long switching times, conversion is very poor, much lower than for the same amount of CSTRs with unidirectional operation and feed at the first CSTR, while at short switching times the conversion is much higher. Notice how a transition window, between of $0.1<\delta\tau^*<1.0$, appears between the two limiting cases at long and short switching times.

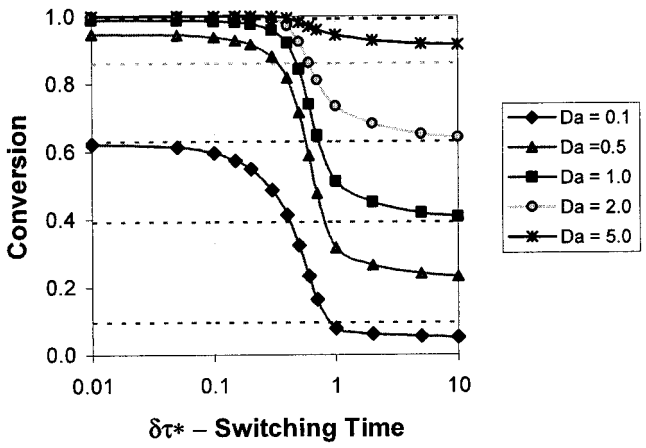

Figure 8. Average conversion in a RFCR (*N=51*) as a function of the switching time for different reactor sizes for the reaction A→B.

The dashed lines show the conversion for 51 CSTRs in series with feed at the first CSTR, and unidirectional flow for the corresponding overall reactor size.

At long switching times, the cycle time is much longer that the time it takes for a pulse of reactant to travel across the reactor and, therefore, the reactor reaches steady-state operation long before the carrier flow direction is reversed. Consequently, the reactor behaves as a series of $^{(N+1)}/_{2}$ CSTRs at steady state with reactant feed at the first CSTR under unidirectional flow. Then, the exit concentration for this case is given by

$$C_{\text{exit}} = \frac{C_0}{(1 + Da_i)^{(N+1)/2}} \tag{22}$$

The conversion given by Eq. 22 is the minimum that can be achieved by a RFCR for given values of *Da* and *N*. This result is independent of whether the reactant adsorbs or not.

The maximum conversion for the RFCR is achieved at short switching times. For this case, the reactor behavior is described by a dispersion-like model. For a finite number of CSTRs, the model can be expressed in matrix form as

$$\mathbf{AC} = \mathbf{F} \tag{23}$$

where

$$\mathbf{A} = \begin{bmatrix} 1+Da & -\frac{1}{2} & & & 0 \\ -\frac{1}{2} & 1+Da & -\frac{1}{2} & & \\ & \ddots & \ddots & \ddots & \\ & -\frac{1}{2} & 1+Da & -\frac{1}{2} & \\ 0 & & & -1 & 1+Da \end{bmatrix} \tag{24a}$$

$$\mathbf{F} = \begin{bmatrix} 0 \\ \vdots \\ 0 \\ C_0 \end{bmatrix} \leftarrow \frac{N+1}{2} \tag{24b}$$

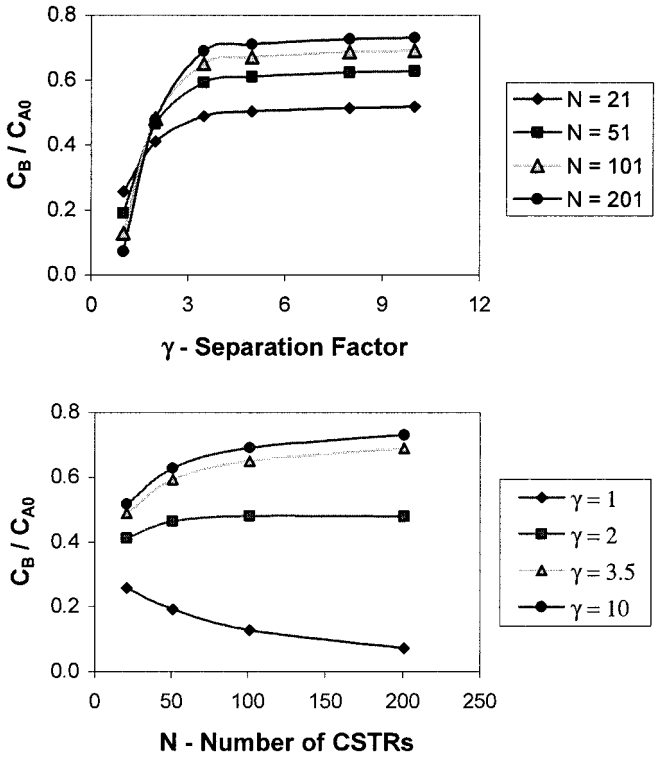

Figure 9. Effect of N and γ on the yield of B for the reaction A→B→C ($\delta\tau^*$=0.4, Da=0.5, and κ=1).

and $\mathbf{C}(1)$ is the exit concentration and $\mathbf{C}(^{(N+1)}/_2)$ is the feed CSTR concentration. Only $^{(N+1)}/_2$ CSTRs are considered since the concentration within the reactor at short switching times is symmetrical with respect to the feed point. As it was the case for long switching times, the mathematical result is independent of the adsorption capacity of the reactant or products.

Consecutive reactions

For every single value of the ratio of kinetic constants κ used in this study, an exit concentration of B exceeding the optimal value for plug-flow reactors (PFR) can be obtained. The optimal value for plug-flow reactor was obtained by selecting the value of Da, that maximized the exit concentration of the intermediate product B. The improvement over the PFR value depends strongly on N and γ. An increase in the difference of the residence time of the species, determined by γ, inhibits the rate of the second reaction by removing B fast enough to prevent a significant conversion of B to C, while maintaining the same conversion of A. The degree of dispersion of the different chemical species is determined by the number of equilibrium stages. Increasing the number of equilibrium stages reduces the dispersion, which increases the conversion of A to B and of B to C. However, since A is better trapped than B, a net increase in the exit concentration of B is predicted as shown in Figure 9. An important observation is that a plateau in the exit concentration of B is observed for $\gamma>5$, while the exit concentration increases logarithmically with the number of equilibrium stages (N).

The last two parameters of the model can be controlled by the design (Da), and by the operation ($\delta\tau^*$) of the reactor. Unlike N and γ, there is a range of Da and $\delta\tau^*$, where the conversion is improved over a PFR and a specific optimal value where conversion is maximized. This range determines the stability and robustness of the system. Figure 10 shows the average exit conversion for a consecutive reaction system with κ=1, γ=5 and N=51. There is a wide range of Da and $\delta\tau^*$, where the plug flow exit concentration is exceeded, showing the robustness and stability of the system. An important feature is that the range where the RFCR improves over the PFR is between $0.1<\delta\tau^*<1.0$, the same range where the irreversible reaction is between the two limiting cases. When $\delta\tau^*$ is large, the residence time of A is not large enough to allow a significant amount of B to be produced. If $\delta\tau^*$ is too small, both A and B are trapped, resulting in formation of the undesired product C, instead of B. The cause for a range of useful Da is simple. For large Da, both reactions tend to go to completion, finally decreasing the amount of B produced, whereas, if the reactor is too small ($Da\rightarrow 0$), then the production of B is limited by incomplete conversion of A.

It was also observed that a larger N resulted in smaller Da, and slightly larger $\delta\tau^*$ at the optimal conversion. The effect of γ on Da for optimal conversion is similar to the effect of N, but it decreases $\delta\tau^*$ at the optimal conversion. These results can be explained by a steeper front of A, and a higher concentration of A within the front, caused by the decrease in the dispersion. The higher concentration of A results in faster reaction rates for A, allowing a decrease in the reactor size, and with it a decrease in the residence time of B, allowing for an increase in the concentration of B. An increase in γ results in shorter $\delta\tau^*$ due to the easier removal of B, and, therefore, the flow direction can be reversed earlier allowing less amount of B to escape while A is still trapped.

Reversible reactions

As for reversible reactions, there is a combination of N, γ, $\delta\tau^*$, and Da that yields conversions exceeding the thermodynamic equilibrium value for every K_{eq}, and it depends strongly on γ and N. Higher conversions are obtained when γ increases since the reverse reaction rate is inhibited by removing the product form the high-reactant concentration zone. Larger val-

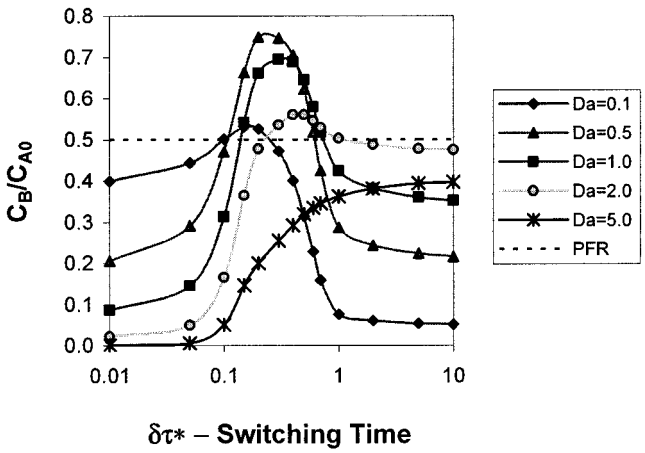

Figure 10. Average yield of B as a function of the switching time ($\delta\tau^*$) with Da as a parameter for the reaction A→B→C (γ=5, N=51, and κ=1).

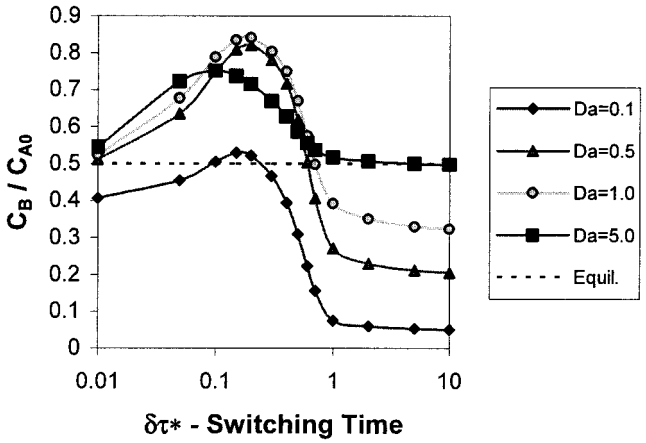

Figure 11. Average exit conversion as a function of the switching time ($\delta\tau^*$) with *Da* as a parameter for the reaction A⇄B (γ=5, *N*=51, and K_{eq}=1).

ues of *N* increase the separation of products and reactants and, consequently, the conversion of the reaction.

Figure 11 shows the range of *Da* and $\delta\tau^*$, where the conversion exceeds the equilibrium value and that a specific optimal value, where conversion is maximized, exists. Again, this wide range of *Da* and $\delta\tau^*$, where the equilibrium conversion is

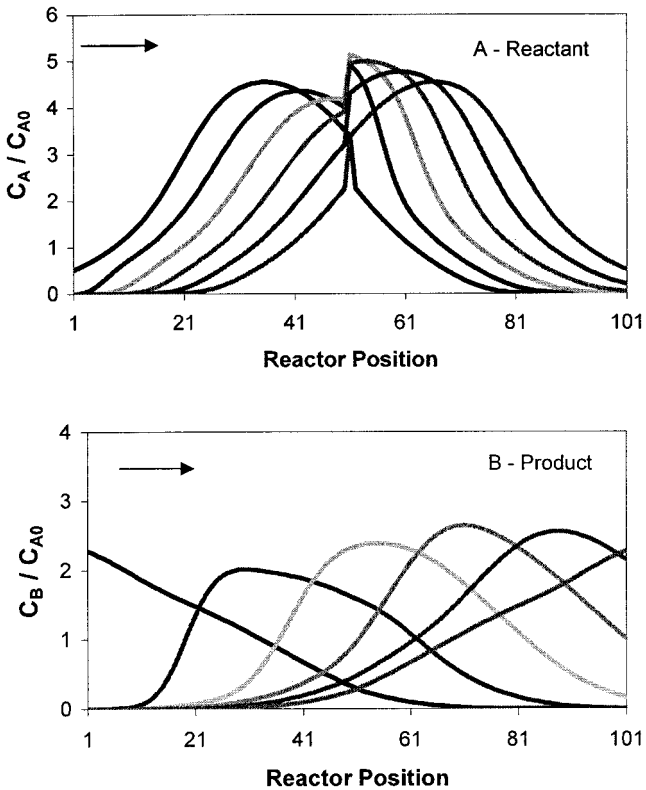

Figure 12. Concentration profiles as a function of time for γ=3.21, K_{eq}=1.63, *N*=101, *Da*=0.75, and $\delta\tau^*$=0.3.

The arrow shows the flow direction.

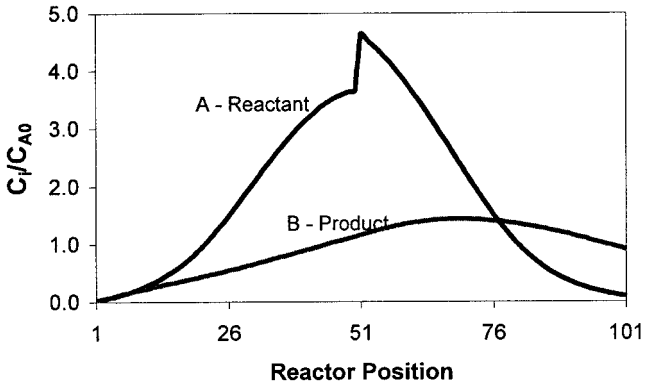

Figure 13. Average concentration profile across half a cycle for γ=3.21, K_{eq}=1.63, *Da*=0.75, $\delta\tau^*$=0.3 and *N*=101.

exceeded shows the robustness and stability of the system. Notice that the improvement in conversion is obtained between $0.01<\delta\tau^*<1.0$. The effect of $\delta\tau^*$ is as follows: long switching times ($\delta\tau^*>1.0$) allow the reactants to escape from the reactor, while very short switching times ($\delta\tau^*<0.01$) not only trap the reactants, but also trap the products. At very long switching times ($\delta\tau^*>>10$), the RFCR shows an asymptotic behavior toward the equilibrium conversion for large reactor sizes. The trapping of the reactant and not the product is clearly seen in Figure 12, where the concentration profile of the RFCR is seen as a function of time.

The range of *Da* where conversion exceeds equilibrium values usually lies between 0.1 and 2.0. As stated earlier in the introduction, if the residence time is too short, no significant reaction will occur despite the high concentration of reactant inside the reactor, whereas, if the residence time is too long, separation of the products will not be sufficient to improve conversion.

The effect of *N* and γ on the optimal values of $\delta\tau^*$, and *Da* is the same as in consecutive reactions, but the cause of this effect is different. The steeper front, and higher concentration of reactant, caused by the increase in *N*, increases the rate of forward reaction and increases the separation between the products and reactants, thus requiring a smaller reactor and

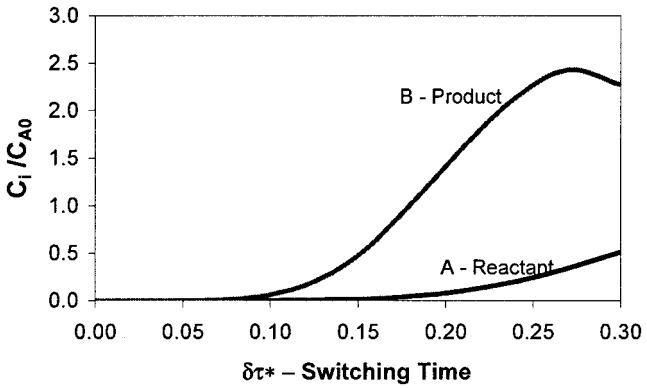

Figure 14. Exit concentration of reactant and products across half a cycle for γ=3.21, K_{eq}=1.63, *Da*=0.75, $\delta\tau^*$=0.3 and *N*=101.

Table 1. Comparison of Reactor Performance

Reactor Type	CMCR*		SCMCR		RFCR
	Experiment	Model	Experiment†	Model‡	Model
Conversion	0.88	0.97	0.83	0.97	0.904
Product purity	0.95	1.00	0.96	0.98	0.904

*Fish and Carr (1989).
† Ray and Carr (1995).
‡ Ray et al. (1994).

allowing longer switching times. Shorter switching times are required when γ increases, because easier removal of the products is obtained and, therefore, the flow direction can be reversed earlier allowing less amount of reactant to escape.

Model reaction results and comparison

In order to compare the RFCR with other types of chromatographic reactors, the hydrogenation 1,3,5-trymethylbenzene (MES) was used as a model reaction. This reaction was chosen because it has been extensively studied in both countercurrent moving-bed chromatographic reactors (CMCR), and, in simulated countercurrent moving-bed reactors (SCMCR), it has pseudo first-order kinetics when the reaction is carried in excess hydrogen, and the reactant adsorbs more strongly than the product in the chromatographic reactor.

The values of γ and K_{eq} for the hydrogenation of 1,3,5-trimethylbenzene (MES) to 1,3,5-trimethylcyclohexane (TMC) were obtained from Ray and Carr (1995), and, with these data (γ=3.21, K_{eq}=1.63), a plot of concentration as a function of switching time with reactor sizes as parameters was obtained. This plot is very similar to that shown in Figure 11, and from there it was found that conversion is optimized for Da=0.75, and $\delta\tau^*$=0.3 yielding in 90.4% conversion. The average concentration as a function of the CSTR number across one-half cycle for the optimum conversion is shown in Figure 13, whereas Figure 14 shows the exit concentration as a function of time for the optimum average conversion. These two figures show how MES is trapped inside the reactor, whereas TMC escapes before the flow direction is changed.

The experimental and model results given by Ray and Carr (1995) are compared to the results of this study in Table 1. Although lower conversions are obtained for the RFCR, the conversion is very close to that of a CMCR and SCMCR with the advantage of the simplicity of the reactor in terms of the number of columns, amount of valves, and control of the system. Consider that the experimental setup for the SCMCR consisted of 4 columns, with multiple exits (one for MES, other for TMC), and multiple flow rates, plus all the different valves, and the computer control required, whereas a RFCR has only two three-way solenoid valves, and one packed bed. The difference between the experimental and model results for the CMCR, and the SCMCR shows the need for experimental verification of the RFCR theory.

Conclusions

For the simple cases presented with isothermal, linear adsorption equilibrium, the RFCR holds great promise to improve conversion beyond thermodynamic equilibrium values where an adsorbent has greater adsorption capacity for the reactant than for the products. Furthermore, the amount of catalyst or the reactor length required to achieve high conversions is dramatically reduced. This improvement is achieved by trapping the reactant inside the reactor, generating a high concentration zone, where reaction proceeds faster, and by having differential residence times that favors the removal of the product, therefore, reducing the reverse reaction rate.

For consecutive reaction systems, the RFCR improves both selectivity and yield over the optimum PFR reactor, while using smaller reactors. This improvement is caused mainly by the differential residence time, achieved by the introduction of an adsorbent that selectively adsorbs the reactant, which favors complete conversion of the main reactant, while reducing the decomposition of the desired intermediate product.

The RFCR has also the advantage that is mechanically simpler than simulated moving-bed chromatographic reactors, it does not have the solid handling problems presented in countercurrent moving-bed reactors, and the pressure and flow variations upstream and downstream of the reactor present for adsorption enhanced reactors, or pressure-swing reactors, are avoided. At the same time, the improvements in conversion and yield or selectivity are maintained.

Notation

V = m^3total reactor volume
q = m^3/scarrier flow rate
t_s s = half cycle time
k_f = s^{-1}forward reaction rate constant
k_r = s^{-1}reverse reaction rate constant
Ki = adsorption equilibrium constant of component i
ε = Void fraction
K_i' = $\varepsilon+(1-\varepsilon)K_i$
γ = K_A'/K_B'
N = number of CSTRs
κ = k_1/k_2, reaction rate ratio
K_{eq} = k_f/k_r, reaction equilibrium constant
Da = k_fV/q, Damkohler Number (reactor size)
τ = tq/VK_A', dimensionless time
$\delta\tau_I$ = t_sqN/VK_A', dimensionless half-cycle time per CSTR
$\delta\tau^*$ = t_sq/VK_A', dimensionless half-cycle time

Literature Cited

Agar, D., and W. Ruppel, "Extended Reactor Concept for Dynamic DeNOx Design," *Chem. Eng. Sci.,* **43** (8), 2073 (1988).

Azevedo, D., and A. Rodrigues, "Design Methodology and Operation of a Simulated Moving Bed," *Chem. Eng. J.,* **82**, 95 (2001).

Barker, P., G. Ganestos,J Ajongwen, and A. Akintoye, "Bioreaction-Separation on Continuous Chromatographic Systems," *Chem. Eng. J.*, **50**, B23 (1992).

Cho, B., R. Carr, and R. Aris, " A Continuous Chromatographic Reactor," *Chem. Eng. Sci.*, **35**, 74 (1980).

Coca, J., and S. Langer, "Doing Chemistry in the Gas Chromatograph," *Chemtech*, **13**, 682 (1983).

Falle, S., J. Kallrath, B Brockmuller, A. Shreieck, J. Griddings, D. Agar, and O. Watzenberger, "The Dynamics of Reverse Flow Chromato-

graphic Reactors with Side Stream Feed," *Chem. Eng. Comm*., **135**, 185 (1995).
Fish, B., and R. Carr, "An Experimental Study of the Countercurrent Moving Bed Chromatographic Reactor," *Chem. Eng. Sci*., **44** (9), 1773 (1989).
Gore, F., "Performance of Chromatographic Reactors in Cyclic Operation," *I&EC Process Des. and Dev.*, **6** (1), 10 (1967).
Kawase, M., T. Suzuki, Y. Inoue, K. Yoshimoto, and K. Hashimoto, "Increased Esterification Conversion by Application of the Simulated Moving Bed Reactor," *Chem. Eng. Sci.*, **51** (11), 2971 (1996).
Kawase, M., Y. Inoue,T. Araki, and K. Hashimoto, "The Simulated Moving Bed Reactor for Production of Bisphenol A," *Catalysis Today*, **48**, 199 (1999).
Kawase, M., A. Pilgrim, T. Araki, and K. Hashimoto, "Lactosucrose Production Using a Simulated Moving Bed Reactor," *Chem. Eng. Sci*., **56**, 453 (2001).
Kruglov, M., Bjorklund, and R. Carr, "Optimization of the Simulated Countercurrent Moving-Bed Chromatographic Reactor for the Oxidative Coupling of Methane," *Chem. Eng. Sci*., **51** (11), 2945 (1996).
Matros, Y. S., *Catalytic Process under Unsteady-State Conditions*, Elsevier Amsterdam (1989).
Matsen, J., J. Harding, and E. Magee, "Chemical reactions in chromatographic columns," *J. of Physical Chemistry*, **69** (2), 522 (1965).
Matsen, J., "Continuous Chromatographic Catalytic Reaction and Separation of Products," *US*., **3**,361 (1968).
Mazzotti, M., A. Kruglov, B. Meri, D. Gelosa, and M. Morbidelli, "A Continuous Chromatographic Reactor: SMBR," *Chem. Eng. Sci*., **51** (10), 1827 (1996).
Mile, B., L. Morton, and P. Sewell, "Yield Enhancement in a Chromatographic Catalytic Reactor," J. *Chem. Soc. Chem. Comm*., 861 (1980).
Petroulas, T., R. Aris, and R. Carr, "Analysis and Performance of a Counter Current Moving Bed Chromatpographic Reactor," *Chem. Eng. Sci*., **40** (12), 2233 (1985).
Ray, A. K., R. Carr, and R. Aris, " The Simulated Counter Current Moving Bed Reactor: A Novel Reactor-Separator," *Chem. Eng. Sci.,* **49** (4), 469 (1994).
Ray, A. K., and R. Carr, " Experimental Study of a Laboratory Scale Simulated Counter Current Moving Bed Chromatographic Reactor," *Chem. Eng. Sci*., **50** (14), 2195 (1995).
Schweich, D., and J. Villermaux, "The Chromatographic Reactor. A New Theoretical Approach," *Ind. Eng.Chem. Fundam*., **17** (1), 1 (1978).
Schweich, D., and J. Villermaux, "Model for the Dehydrogenation of Cyclohexane in a Chromatographic Reactor: Comparison of Theory and Experience," *Ind. Eng. Chem. Fundam*., **21**, 47 (1982).
Takeuchi, K., and Y. Uraguchi, "Basic Design Procedure of Chromatographic Moving-Bed Reactor for Product Refining," *Chem. Eng. J. Japan*, **9** (3), 246 (1976).
Takeuchi, K., and Y. Uraguchi, "The effect of the Exhausting Section on the Performance of a Chromatographic Moving-Bed Reactor," *Chem. Eng. J. Japan*, **10** (6), 72 (1977).
Takeuchi, K., and Y. Uraguchi, "Experimental Studies of a Chromatographic Moving-Bed Reactor. Catalytic Oxidation of Carbon Monoxide in Activated Alumina as a Model Reaction," *Chem. Eng. J. Japan*, **10** (6), 455 (1977).

Manuscript received Jan. 9, 2003, and revision received Jan. 9, 2004.